Supplementary Materials:

Isaac Kwesi Nooni[1], Faustin Katchele Ogou [2], Abdoul Aziz Saidou Chaibou [3], Francis Mawuli Nakoty [4], Gnim Tchalim Gnitou [5] and Jiao Lu[1,*]

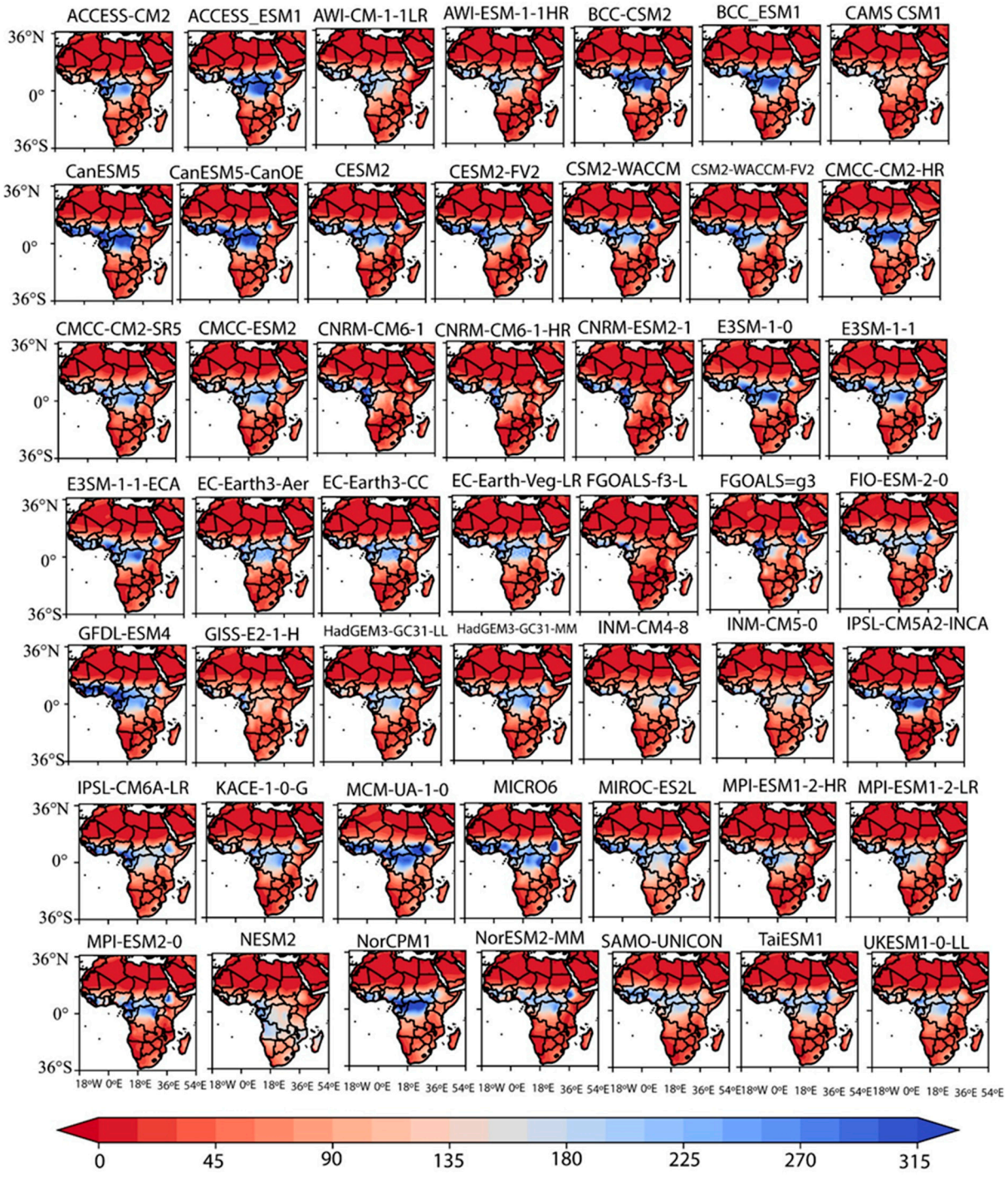

Figure S1. Spatial distribution of MJJASON mean precipitation in selected 49 during 1980-2014. The unit is mm year^{-1}.

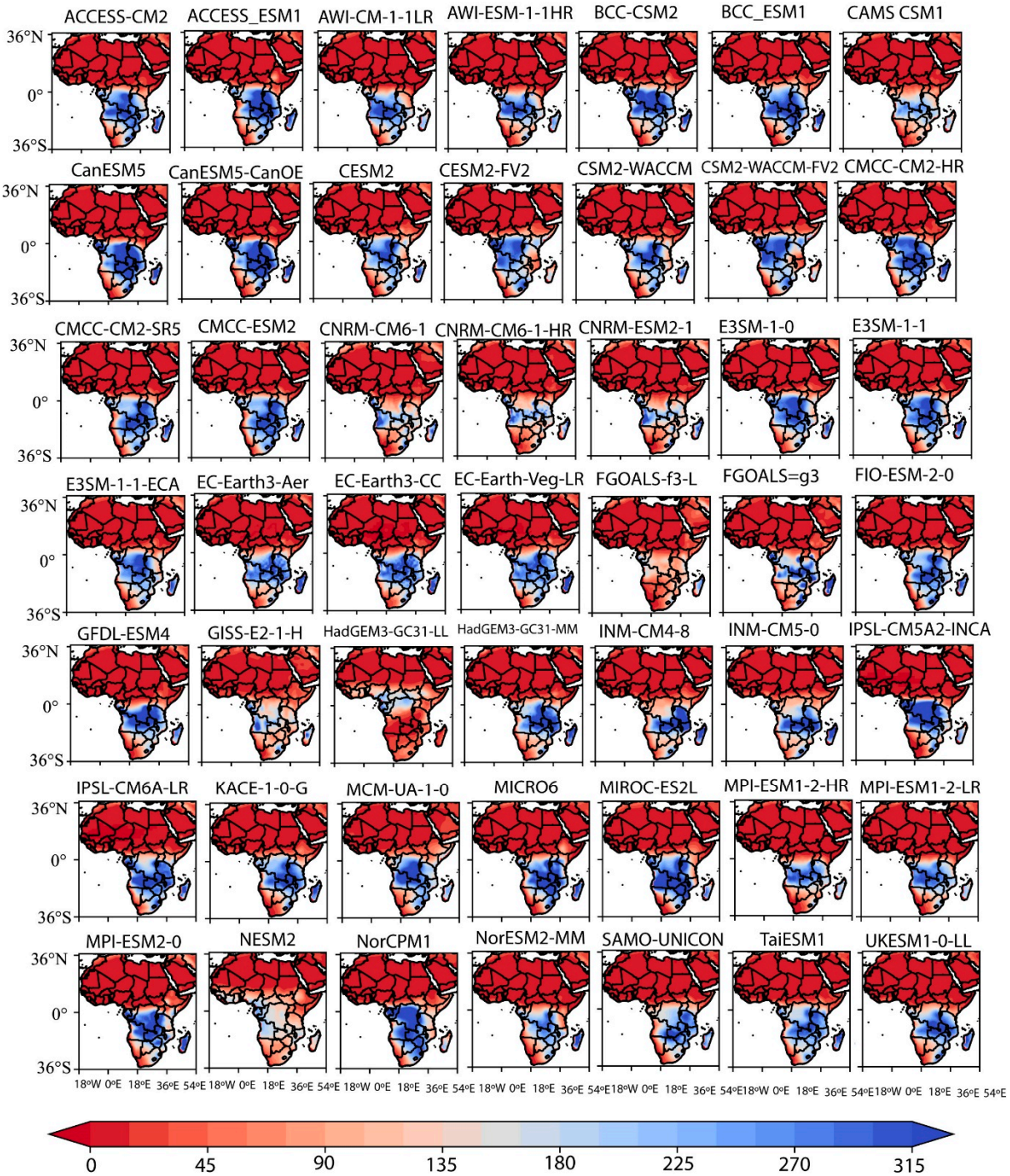

Figure S2. Spatial distribution of DEC mean precipitation in selected 49 during 1980-2014. The unit is mm year^{-1}.

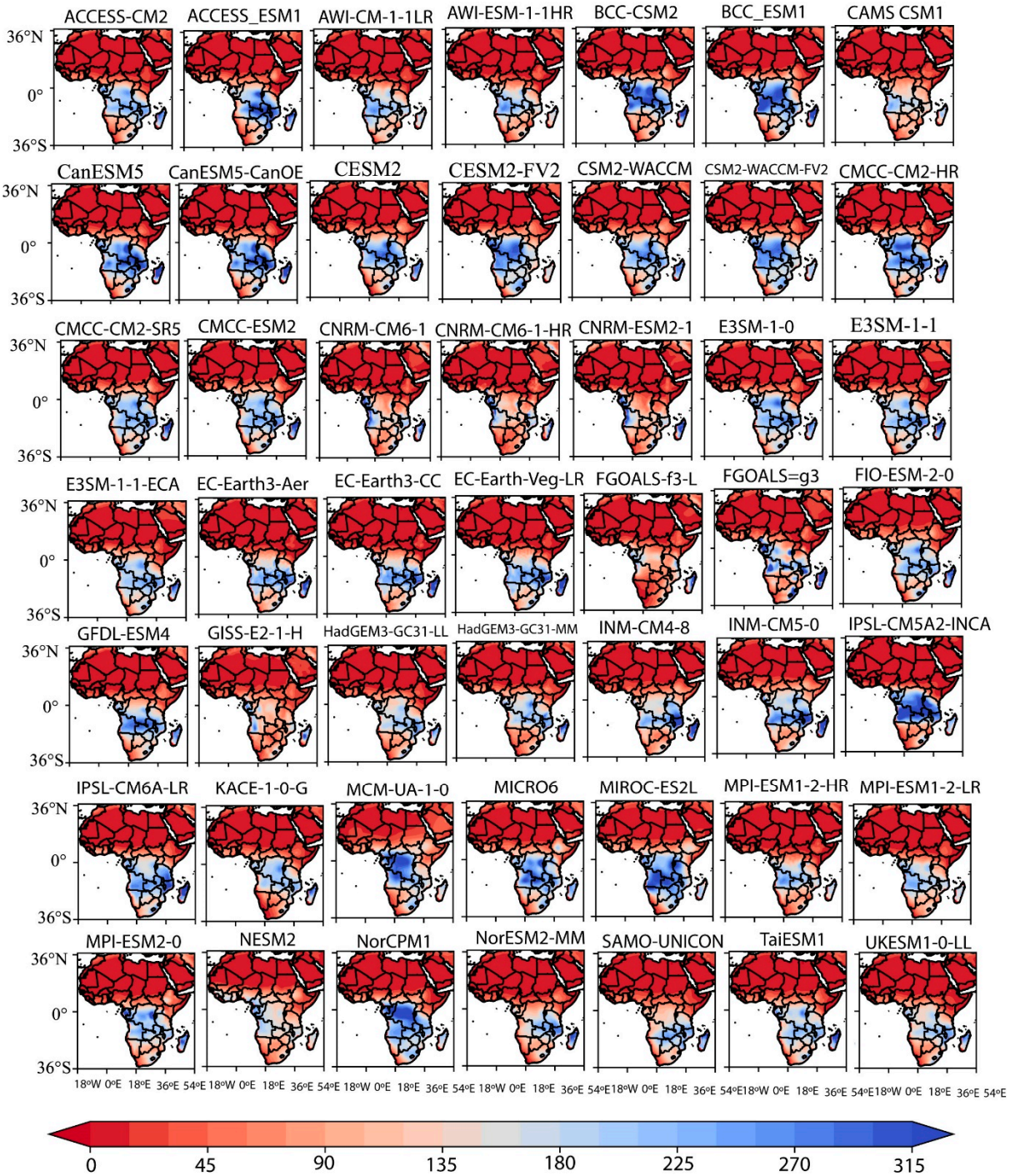

Figure S3. Spatial distribution of JFMA mean precipitation in selected 49 during 1980-2014 The unit is mm year^{-1}.

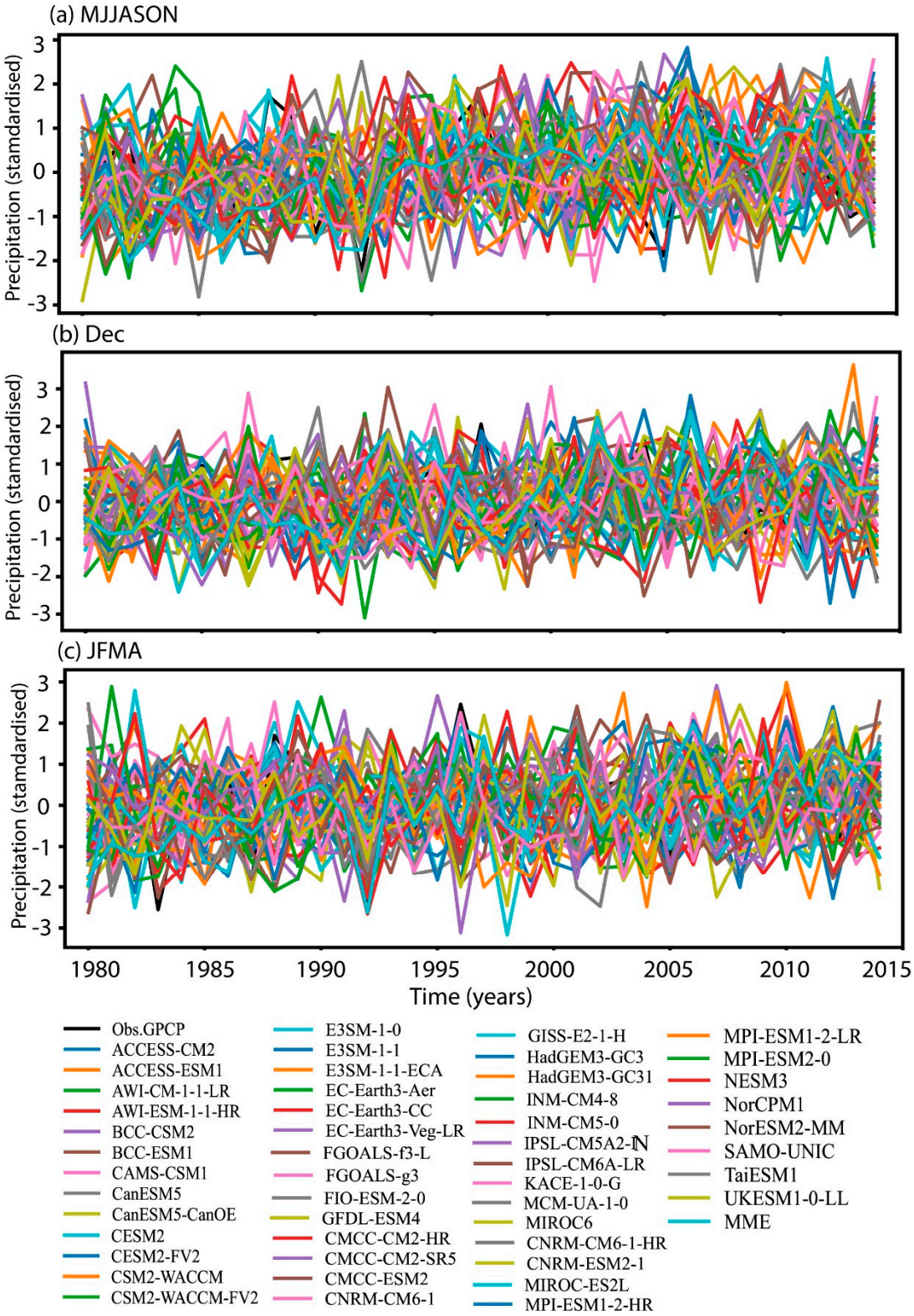

Figure S4. Seasonal variations of observation (i.e., GPCP, black line) CMIP6 MMM and 49 CMIP6-simulated precipitation anomalies during 1980 to 2014 across Africa and Arabian Peninsula. Anomalies are calculated with respect to the mean over the period.

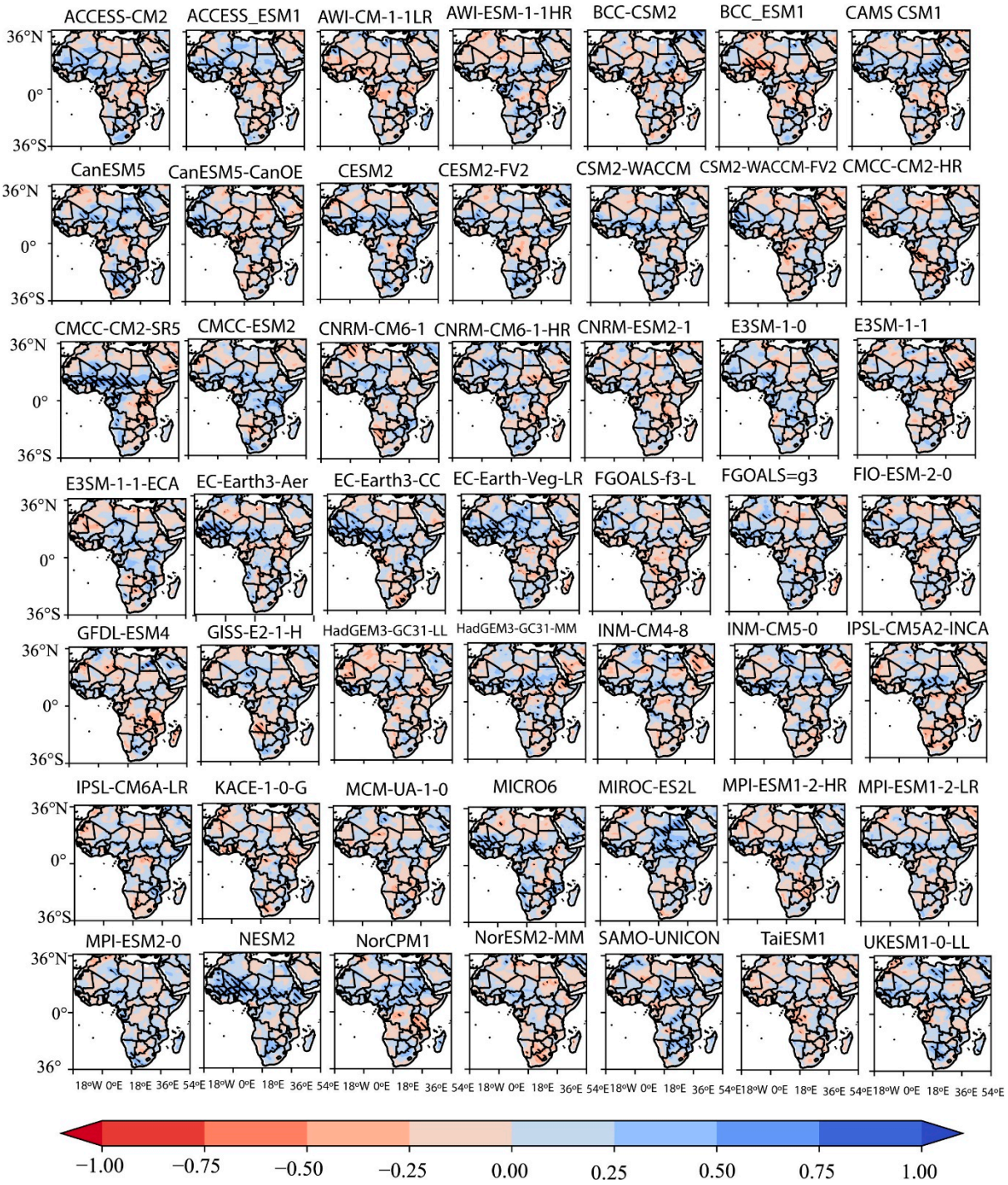

Figure S5. Spatial distributions of correlation coefficients of 49 selected CMIP6 models and SST during 1980-2014 at MJJASON. Hatched area indicates 95% confidence level.

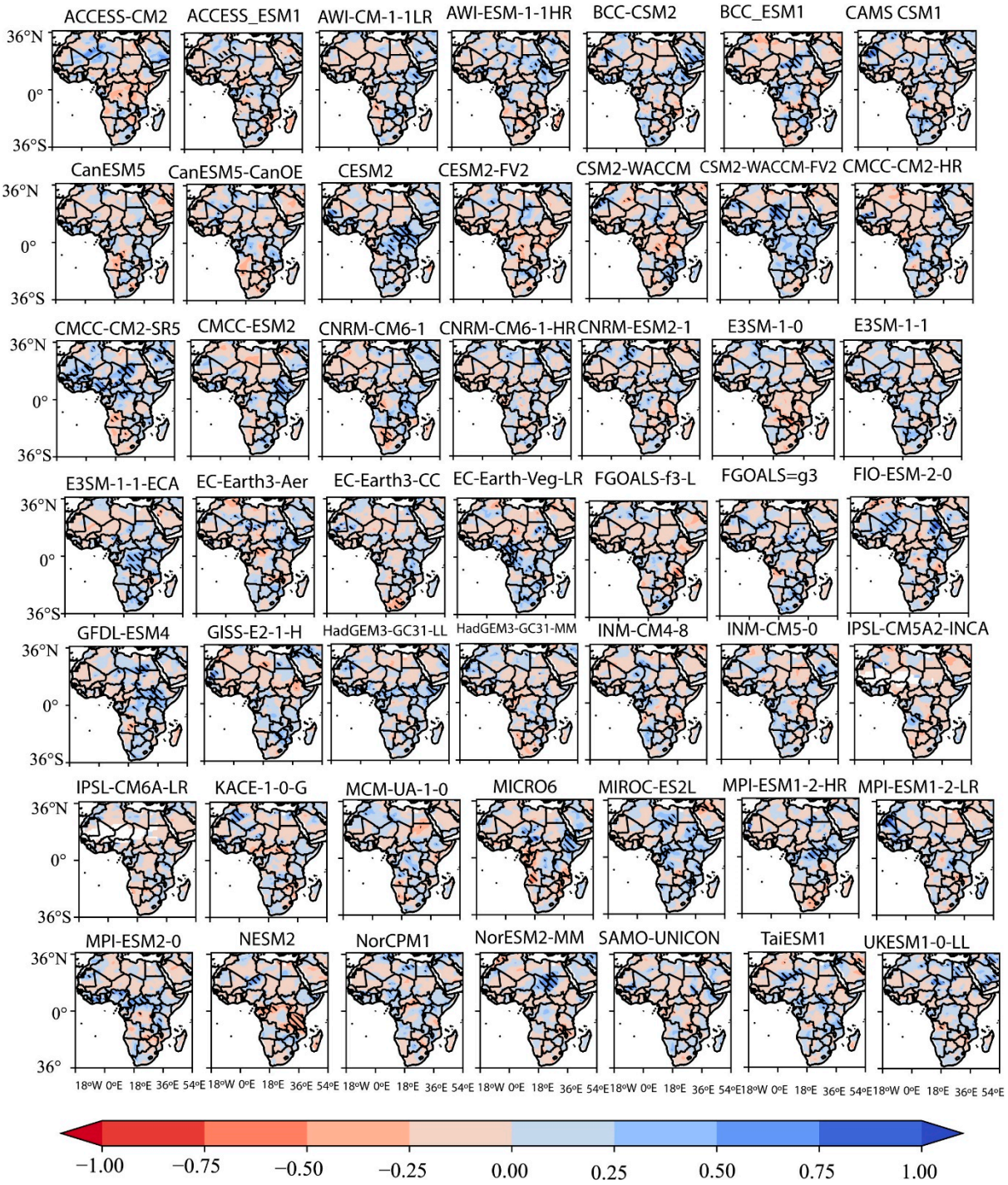

Figure S6. Spatial distributions of correlation coefficients of 49 selected CMIP6 models and SST during 1980-2014 at December. Hatched area indicates 95% confidence level.

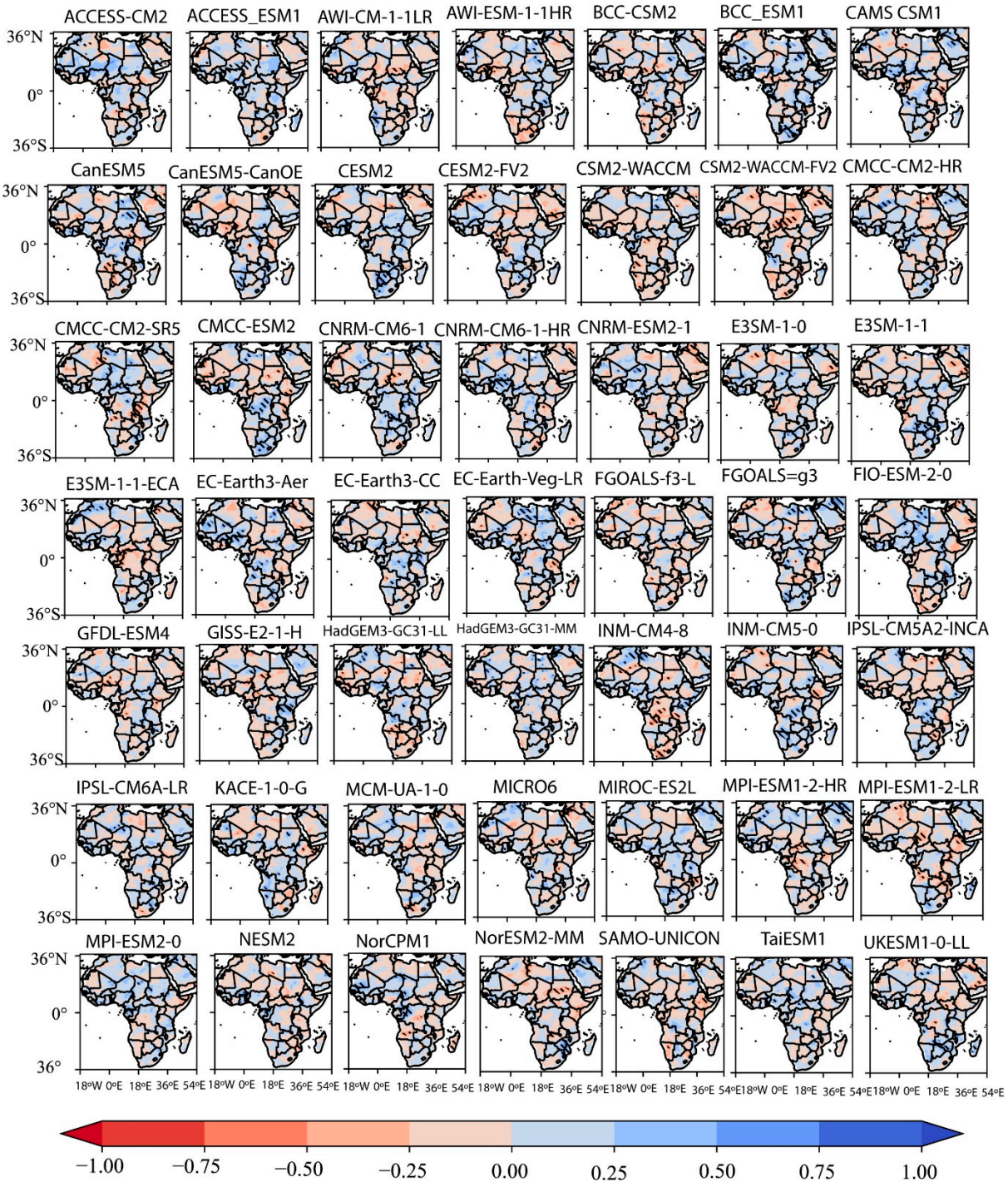

Figure S7. Spatial distributions of correlation coefficients of 49 selected CMIP6 models and SST during 1980-2014 at JFMA. Hatched area indicates 95% confidence level.

Table S1 Individual models at different temporal scales showing high degree of scattering (SD) higher than the CMIP6 MME.

Models	**SD at annual**	**Models**	**SD (MJJASON)**	**Models**	**SD (JFMA)**
E3SM-1-1	1.54	MPI-ESM2-0	1.76	E3SM-1-1-ECA	1.94
INM-CM5-0	1.54	IPSL-CM6A-LR	1.78	E3SM-1-1	1.95
FIO-ESM-2-0	1.56	CMCC-CM2-SR5	1.79	FIO-ESM-2-0	1.96
KACE-1-0-G	1.56	CESM2-FV2	1.81	EC-Earth3—Aer	1.97
TaiESM1	1.57	CESM2	1.82	INM-CM4-8	1.98
CSM2-WACCM	1.59	CSM2-WACCM	1.82	MPI-EM2-0	1.98
E3SM-1-1-ECA (1).	1.59	CSM2-WACCM-FV2	1.84	EC-Earth3-CC	2.03
CESM2	1.60	E3SM-1-1ECA	1.80	CSM2-WACCM	2.04
FGOALS-g3 (),	1.60	NESM3	1.87	FGOALS-g3	2.04
MPI-ESM2-0	1.61	E3SM-1-0	1.88	GFDL-ESM4	2.05
CMCC-ESM2	1.65	MICROC-ES2L	1.90	CESM2	2.07
E3SM-1-0	1.65	CMCC-CM2-HR	2.01	CMCC-CM2-SR5	2.08
CMCC-CM2-SR5	1.66	BCC-ESM1	2.05	CMCC-ESM2	2.07
NESM3	1.67	NorCPM1	2.06	E3SM-1-0	2.07
CSM2-WACCM-FV2	1.67	BCC-CSM2	2.09	ACCESS-ESM1	2.17
CESM2-FV2	1.7	IPSL-CM5A2-INCA	2.08	INM-CM5-0	2.12
IPSL-CM6A-LR	1.71	ACCESS-ESM1	2.16	EC-Earth3-Veg-LR	2.07
GFDL-ESM4	1.78	GFDL-ESM4	2.23	CSM2-WACCM-FV2	2.19
ACCESS-ESM1	1.86	CanESM5-CanOE	2.23	CESM2-FV2	2.25
CMCC-CM2-HR	1.87	CanESM5	2.24	CMCC-CM2-HR	2.27
IPSL-CM5A2-INCA	1.91	MCM-UA-1-0	2.31	IPSL-CM6A-LR	(2.27
BCC-CSM2	1.93			NESM3	2.29
BCC-ESM1	1.94			CanESM5-CanOE	2.30
CanESM5-CanOE	1.94			BCC-CSM2	2.31
MICRO-ES2L	1.96			CanESM5	2.37
CanESM2	1.97			BCC-ESM1	2.39
NorCMM1	2.04			NorCPM1	2.48
MCM-UA-1-0	2.07			IPSL-CM5A2-INCA	2.53
				MCM-UA-1-0	2.26
				MICRO-ES2L	2.51

Table S2. Individual models at different temporal scales showing a low degree of scattering (SD) higher than the CMIP6 MME.

Models	**Standard Deviation (SD) at MJJASON scale**	**Models**	**Standard Deviation (SD) at JFMA scale**
EC-Earth3-Veg-LR	1.65	ACCESS-CM2	1.86
KACE-1-0-G	1.63	KACE-1-0-G	1.77
EC-Earth3-Aer	1.63	SAMO-UNICON	1.76
FGOALS-g3	1.61	AWI-CM-1-LR	1.76
NorESM2-MM	1.60	HadGEM3-GC31-LL	1.69
CNRM-CM6-CM6-1	1.59	NorESM2-MM	1.69
CNRM-ESM2-1	1.58	UKESM1-0-LL	1.69
HadGEM3-GC31-MM	1.58	MPI-ESM1-2-LR	1.68

ACCESS-CM2	1.56	AWI-ESM-1-HR	1.66
AWI-CM-1-1-LR	1.53	CNRM-CM6-1	1.60
UKESM1-0-LL	1.48	CNRM-ESM2-1	1.54
HadGEM3-GC31-LL	1.47	HadGEM3-GC31-MM	1.54
INM-CM4-8	1.46	MPI-ESM1-2-HR	1.65
MPI-ESM1-2-LR	1.47	CNRM-CM6-1-HR	1.50
MPI-ESM1-2-HR	1.46	CAMS-CSM1	1.47
), AWI-ESM-1-HR	1.45	GISS-E2-1-H	1.32
INM-CM5-0	1.43	MICRO6	1.32
CNRM-CM6-1-HR	1.42	FGOALS-f3-L	1.22
MIROC6	1.23		
GISS-E2-1-H	1.23		
CAMS-CSM1	1.17		
FGOALS-f3-L	1.13		